

A new framework for accessing and visualizing Ocean Color Data for Water quality parameter analysis

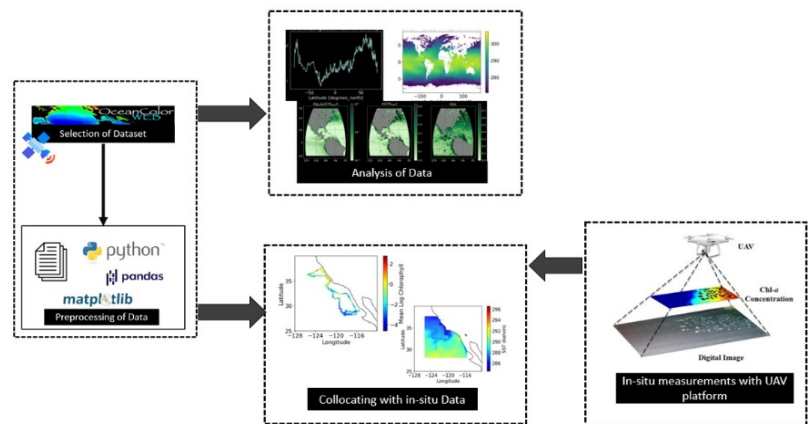
Ashwini M. Deshpande,* Elice Priyadarshini, Aishwarya More, Shreya Pate

Electronics and Telecommunication Department, MKSSS's Cummins College of Engineering for Women, Pune, Maharashtra, India

Received on: 19-June-2023, Accepted and Published on: 16-Aug-2023

ABSTRACT

This paper presents a framework for the remote processing and quantitative analysis of water quality parameters, specifically chlorophyll and sea surface temperature (SST). The framework is organized into three directories. The first directory accesses and examines water quality parameters, the second collocates in-situ observations with satellite data, and the third integrates Ocean Observatories Initiative (OOI) data via Machine to Machine (M2M) interfaces. The analysis of chlorophyll concentration is defined in correlation with SST, employing the Gradient of Mean and Mean of Gradient mathematical tools for change detection. The result is a system that leverages cloud technology to access, process, and analyze data. With a spatial gradient tolerance of 90 percentile, the framework enables accurate change detection from time-average data. This methodology contributes to the field of water quality analysis, offering new insights into environmental monitoring and marine science.



Keywords: Water quality parameters, Chlorophyll, Sea Surface Temperature (SST), Remote processing, Ocean Observatories Initiative (OOI), Machine to Machine (M2M), Gradient of Mean, Mean of Gradient, Cloud technology, Change detection.

INTRODUCTION

Water quality is subject to constant change due to a myriad of factors including natural phenomena (e.g., weather, rainfall) and human activities (e.g., industrial discharges, accidental spills).^{1,2} The effective monitoring of these changes is vital for the sound management of water resources.^{3,4} Remote sensing offers an efficient, methodical approach for monitoring and analyzing large, outlying, and otherwise inaccessible locations. This technology enables spatial and temporal analysis across vast regions, offering a cost- and time-effective solution.⁵ Major challenges in the studies of remote sensing data and diverse set of applications including environmental modeling, are discussed by Dubovik et al.⁶ Similarly

the study presented by B. Zhang et al.⁷ bring up how to address some of the hurdles and fully utilize the potential of intelligent remote sensing satellite systems across diverse applications.

Remote sensing methods for water quality parameter analysis involve measuring various factors that determine water quality within specific regions over time, using earth observatory images. This approach has broad applications, such as the development of management plans for various natural resource management issues.⁵ Timely and efficient detection of changes is central to this process. Recent advancements have led to the creation of many remote sensing modular tools for processing satellite imagery for societal and environmental welfare. However, most of these tools necessitate separate downloading and importing of data, sometimes requiring pre-processing before utilization.

Earlier works on the acquisition and analysis of chlorophyll data have emphasized the importance of analyzing harmful algal bloom (HAB) cover with in-situ data, but this can be costly and labor-intensive. Collecting data from remote or extensive areas can be impractical or unfeasible. Therefore, using remote sensing data analysis, an algorithmic approach can be developed to time-

*Corresponding Author: Ashwini M. Deshpande, E&TC Department, Cummins College of Engineering for Women, Pune
Email: ashwini.deshpande@cumminscollege.in

Cite as: J. Integr. Sci. Technol., 2024, 12(1), 707.

©Authors; ScienceIN ISSN: 2321-4635
http://pubs.thesciencein.org/jist

correlate ocean color data.^{8,9} In this work, we utilized open-source satellite data from the National Aeronautics and Space Administration (NASA)¹⁰ and computed gradients for accurate analysis of chlorophyll growth across vast geographical extents.

The data employed in this method originates from the MODIS (Moderate Resolution Imaging Spectroradiometer) Aqua (formerly EOS PM) satellite for water surface analysis. These NetCDF¹¹ (Network Common Data Form) file formats facilitated the targeting of specific data files in the satellite data download library. We applied a default chlorophyll algorithm (chlor_a), the standard OC3/OC4 (OCx) band ratio algorithm combined with the color index (CI)¹⁰, for detecting chlorophyll from satellite data. The results were then correlated with the Sea Surface Temperature (SST) of the same location, and cross-verified with in-situ Unmanned Surface Vehicle (USV) data from Sairdron Cruise using Python's numpy, matplotlib, pandas, cmocean, and Xarray¹² libraries.

The current framework encompasses:

- Time-variant chlorophyll data plotting after pre-processing and subsetting.
- Normal distribution plotting of processed chlorophyll values through satellite data.
- Comparison of chlorophyll values with SST, including gradient plotting.
- Collocation of processed satellite data with in-situ values using Linear Interpolation and Nearest Neighbor Interpolation methods.

Remote sensing has emerged as a vital tool for identifying and monitoring areas affected by water contaminants, tracking their dispersion patterns through satellite data. Many researchers have contributed to the development of methods for defining and estimating water quality parameters.¹³

Z. Chen et al. conducted a case study in Tampa Bay, employing time-series images from MODIS, collected over a four-year span, for mapping turbidity.¹⁴ They developed a method for turbidity mapping, comparing it with in-situ surveys, and concluded that satellite remote sensing is an invaluable tool for water quality monitoring. This approach enhanced the assessment of turbidity patterns within their study.

Gholizadeh et al.¹⁵ conducted an extensive review of water quality parameter estimation, recommending hyperspectral remote sensing on platforms such as Landsat-8 for local studies.

G. Yang et al.¹⁶ utilized MODIS surface reflectance data, specifically products like MOD09GQ and MYD09GQ, to derive water surface turbidity in Darwin Harbour and adjacent coastal areas. This application of MODIS surface reflectance products has demonstrated its utility in this context.

In another dimension of marine pollution detection, a comprehensive analysis encompassing oil spill identification, algal bloom monitoring, and river plume tracking using active spaceborne sensors was presented in ref^[13]. Shen et al. proposed a specific framework to study harmful algal blooms through remote sensing.¹⁷ Additionally, a critical review focusing on phytoplankton blooms and the application of ocean color remote sensing methods was detailed in work reported in ref^[18].

Chauhan et al.¹⁹ contributed to understanding chlorophyll distribution on the sea surface, based on Ocean Colour Monitor satellite data obtained from IRS-P4. Whereas, the research conducted by Shareef et al. assessed and monitored water quality by utilizing texture parameters such as Gray-Level Co-Occurrence Matrix (GLCM).²⁰ They employed a polynomial quadratic model to fit, measure, and calculate water quality parameters, achieving an accuracy of up to 95%.

Chiswell et al. embarked on an intricate climatology study of mean and seasonal cycles, carefully exploring their spatial extent and timing as key factors.²¹ This investigation laid the groundwork for further exploration of water quality parameters such as chlorophyll concentration and sea surface temperature (SST). In a related vein, Brown and Minnet devised an algorithm using MODIS to observe SST, investigating the variations in thermal infrared and mid-infrared effects on the back-scattering coefficient between day and night.²² Their work not only extended the understanding of these dynamics but also thoroughly examined the constraints and limitations of remote sensing in lakes and rivers.

Building on these foundational studies, A. G. O' Carroll et al. penned a comprehensive white paper that covered a wide array of aspects related to SST, including its significant impact on climatic patterns.²³ This work further highlighted the future needs for a high-resolution SST observing system and elaborated on methods for water surface temperature retrieval from single-band Landsat imagery through the MODTRAN model, as well as techniques for estimating cloud fraction over water pixels using OLI data.²⁴

Further bridging the gap between satellite observation and actual measurements, J. Vazquez-Cuervo et al. presented the work that validated remotely sensed SST and sea surface salinity (SSS) data against measurements from an unmanned surface vehicle called Sairdron during a campaign in Baja California.^{25,26} Their findings revealing nuanced biases and root mean square differences between various satellite-derived products and USV-derived values, underscored the precision and potential biases in current remote sensing techniques.

In addition to these works, Q. Cao et al.²⁷ discusses the use of hyperspectral remote sensing for inland water quality detection. The authors compare the relative merits of varying remote sensing platforms, popular inversion models, and the application of hyperspectral monitoring of various water quality parameters. The work suggests that with the rapid development of aerospace technology and near-surface remote sensing, the spectral resolution of remote sensing imaging technology has been dramatically improved and has begun to be applied to small water bodies.

These studies showed that remote sensing is a powerful tool for monitoring water quality. It can provide high spatial and temporal resolution data for thousands of lakes at a time, and can be used to evaluate environmental problems and potential health risks through the analysis of changes in water quality and the detection of harmful algal blooms. Remote sensing of water quality involves the use of visible and infrared portions of the electromagnetic spectrum to explore the sensitivity of spectral band combinations by utilizing advanced computing techniques.

There are several open-source software tools available for processing satellite data for water quality monitoring. One such tool is NASA's SeaDAS software, which is used for image processing

and analysis of ocean color data.²⁸ Another tool is Google Earth Engine, a cloud-based platform that supports simple image retrieval and large-scale processing.²⁹ There are also several open-source Python libraries available for working with satellite and aerial imagery data, such as GDAL, Rasterio, and Geopandas.³⁰

By synthesizing these diverse insights and methodologies, the current study has recognized the heavy reliance on parameters such as chlorophyll concentration, SST, and turbidity in existing methods for assessing water quality. Thus, the necessity of developing a well-defined framework that leverages open-source software platforms, such as Python 3.7 (with the gdal and geopandas packages) and SeaDAS 7.5.3 (<https://seadas.gsfc.nasa.gov/downloads/>), emerges. This framework aims to facilitate access to these vital parameters from remotely sensed data, allowing for detailed processing and comparison with in-situ observations over time. Utilizing satellite data from sources like Landsat, Sentinel 1A and 1B, and MODIS (Aqua and Terra), this approach shows promise in enhancing the understanding of regional changes in water parameters, offering a robust avenue for continued exploration and application in water quality analysis.

METHODOLOGY

The main objective of this work is to provide a new framework for full-length processing of satellite images for the determination of water quality parameters analysis. Figure 1 illustrates the complete framework proposed to implement this work, with the description of each block provided in the subsections that follow.

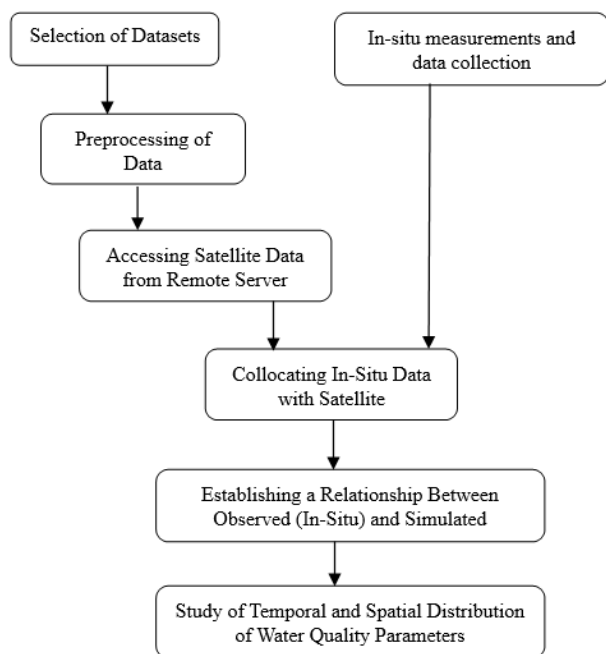


Figure 1. Designed framework for determination of water quality parameters

Accessing Satellite Data From A Remote Server

The retrieval of satellite data constitutes an essential phase in the analytical framework for assessing oceanic parameters, such as

chlorophyll concentration. The data utilized in this study were extracted from NASA's Oceandata.sci 3 Modis Aqua L3SMI, an open-source repository that hosts ocean color data. These datasets are devoid of a time dimension, necessitating a specialized approach for integration into a temporal analysis.

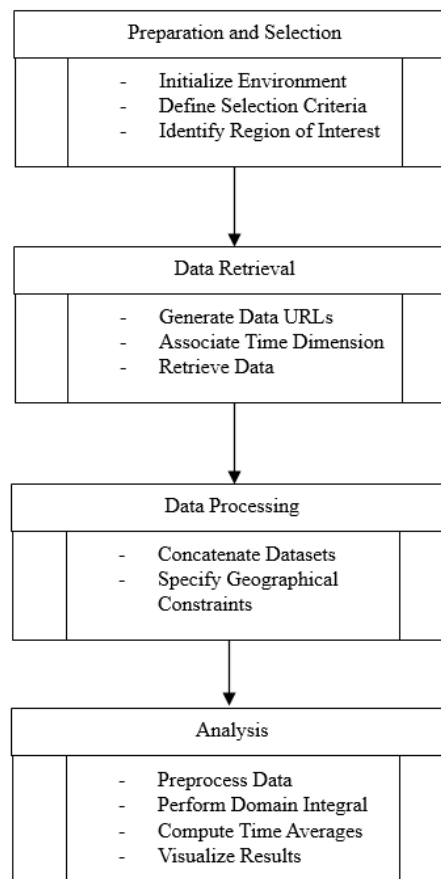


Figure 2. Flowchart for chlorophyll data retrieval from from Cloud Defining the Toolkit for Data Extraction

A systematic toolkit was developed to streamline the extraction of data, encompassing the following specifications for data selection:

- (i) Start Date: The commencement point of the time series.
- (ii) End Date: The concluding date of the time series.
- (iii) Desired Variable: The specific oceanic parameter under study (e.g., chlorophyll concentration).
- (iv) Associated Variable Algorithm/Method: Algorithm used for the particular variable (e.g., chl_ocx algorithm).
- (v) Time-Binning Period: The temporal aggregation level for the data (e.g., 8-day intervals).
- (vi) Spatial Resolution: The granularity of spatial data (e.g., 9 kilometers).

Figure 2 illustrates the process for retrieving chlorophyll data from the cloud. The process begins with the definition of parameters including start and end dates (01-01-2018 to 01-07-2018), desired variable (chlorophyll), algorithm (chl_ocx), time-binning period (8 days), and spatial resolution (9 km). The data is

then retrieved and undergoes cleaning and organization, which includes time alignment and concatenation of individual datasets into a time series dataset. Subsequent mathematical analyses include the computation of time-variable chlorophyll concentrations and spatial distribution.

A time and longitude mean of chlorophyll is computed using the chl_ocx algorithm and visualized in Figure 3. By averaging over both time and longitude, this representation encapsulates the spatial distribution of chlorophyll concentration across latitudes. It helps in revealing patterns and trends that might be linked to geographical features, ocean currents, or seasonal changes. Analyzing such data assists in understanding the ecological dynamics and health of the marine ecosystem.

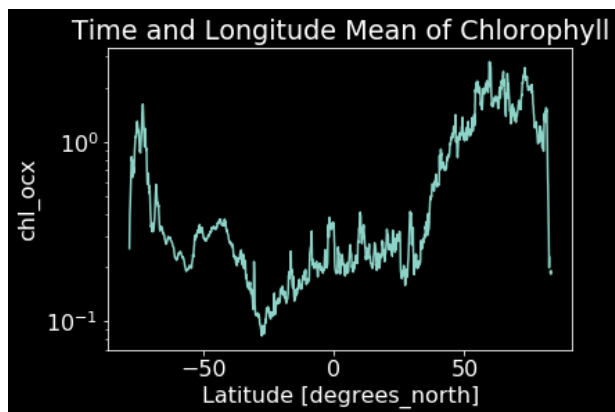


Figure 3. Time and longitude mean of chlorophyll using chl_ocx algorithm

In Figure 4, a plot of the latitude-longitude mean of chlorophyll-a readings obtained from ocean color data is presented. By collapsing the spatial dimensions into a single mean value for each time step, this plot emphasizes the temporal dynamics of chlorophyll concentration. It provides insights into how chlorophyll levels vary over time, independent of specific geographical locations. Such an analysis is crucial for studying phenomena like algal blooms and assessing the impacts of climatic or human-induced changes on marine productivity.

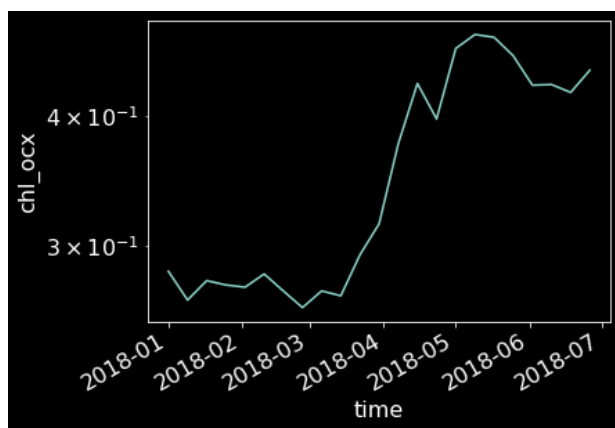


Figure 4. Latitude and longitude mean of chlorophyll using chl_ocx algorithm

In Figure 5, three interconnected visualizations represent different aspects of chlorophyll concentration in the chosen geographical region:

Mean Chlorophyll Concentration (log-transformed): The first plot provides a logarithmic view of the mean chlorophyll concentrations. By utilizing a logarithmic transformation, it emphasizes the differences between areas of low and high concentrations. This highlights the regions where the chlorophyll concentration is more prominent, aiding in identifying areas of ecological interest.

Standard Deviation of Chlorophyll Concentration: The middle plot illustrates the standard deviation (σ) of the chlorophyll concentration across the region. The presentation of standard deviation offers insights into the variability of chlorophyll levels, revealing areas where fluctuations are more significant. This can be indicative of underlying ecological dynamics and may signal areas that warrant further investigation.

Coefficient of Variation (CV) of Chlorophyll Concentration: The third plot represents the coefficient of variation, calculated as the ratio of the standard deviation to the mean. By depicting the CV, it offers a standardized view of the variability relative to the mean concentration. This normalized measure allows for a more direct comparison between different regions and may help in identifying zones where the relative variability is especially noteworthy.

These plots are aligned along meridians and parallels, reflecting their spatial distribution on the Earth's surface. Together, they offer a multi-faceted view of chlorophyll distribution in the study area. By presenting mean concentrations, variability, and relative variability (CV), these visualizations facilitate a nuanced understanding of chlorophyll patterns and their potential ecological significance. This combination of visualizations underscores the complexity of the distribution and may guide further studies to uncover the underlying biological, chemical, and physical processes that govern chlorophyll distribution in the selected region.

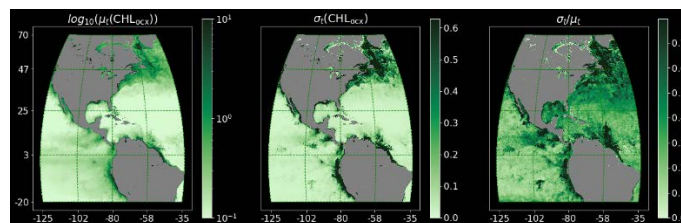


Figure 5. Analysis of Chlorophyll concentration across specified Meridians and Parallels.

Mean Gradient Computation For Chlorophyll And Sea Surface Temperature

The analysis of chlorophyll concentration and Sea Surface Temperature (SST) in oceanographic studies requires the computation of spatial gradients to provide insights into changes and variations across the study region. Figure 6 presents a flowchart outlining the method employed to compute these spatial gradients.

The computation of spatial gradients ($|\nabla \text{chl}|$) for chlorophyll data and corresponding Sea Surface Temperature (SST) is executed through a process that includes several intricate steps, aided by a

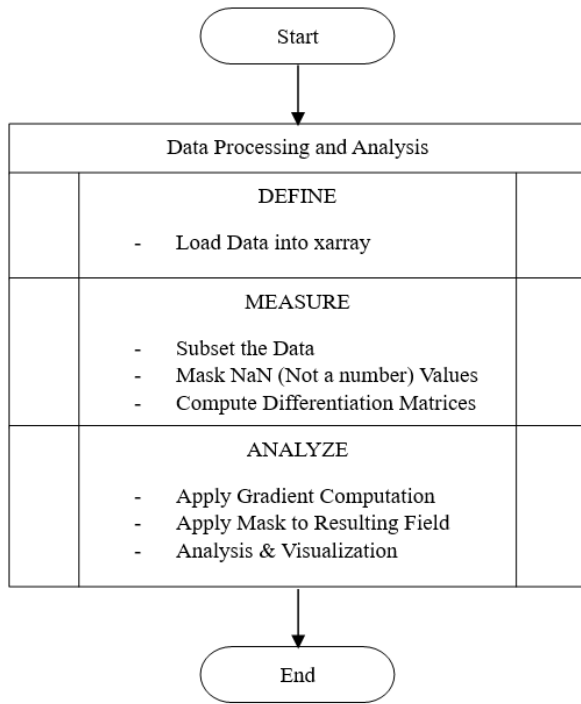


Figure 6. Flowchart for computing spatial gradients

specific toolkit for deriving derivatives. The data is loaded into an x-array format, a strategic decision that enables data transfer to the local machine only when needed. Although this approach minimizes memory requirements, it might lead to an extended computation time. The following key steps are performed:

(i) Data Subsetting: The data is subset to target specific regions of interest, thus reducing the computational load. Figure 7 illustrates this subsetting by showing plots of chlorophyll and SST against the time mean.

(ii) NaN Value Masking: Any NaN (not a number) values within the data set are masked out. This step is essential as NaN values can propagate inaccurately through mathematical operations, especially matrix multiplication, leading to potentially erroneous results.

(iii) Differentiation Matrices Computation: Matrices for differentiation are computed in accordance with the physical grids' spherical coordinates. This step ensures that the spatial characteristics of the data set are appropriately represented.

(iv) Gradient Computation and Masking: The computation of the gradient is applied, and the resulting field is masked consistently with the original data. This uniformity ensures that the masking process aligns with the particularities of the data set, preserving the integrity of the analysis.

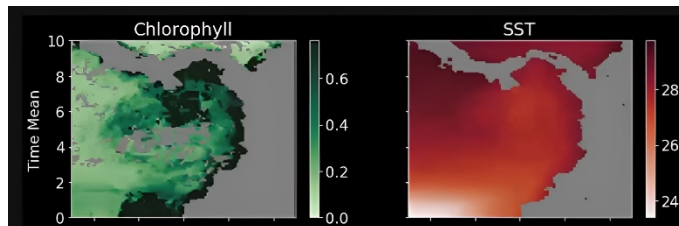


Figure 7. Subset of Chlorophyll and Sea Surface Temperature against time mean

Subsequently, we undertook a comparative analysis of the mean gradient using two distinct approaches: (a) mean of gradient $|\overline{\nabla chl}|$ and (b) gradient of mean $|\nabla \overline{chl}|$, as depicted in Figure 8 (a) and (b) respectively. The objective of this comparison was to assess potential variations between these two approaches and their implications for the dataset.

In theory, both of these approaches should yield identical values. However, due to the presence of missing data points, arising from land or cloud-covered regions, disparities emerge between them. These missing data points introduce errors into the analysis, potentially affecting the accuracy of results.

To address this challenge, we employed an averaging technique to modify certain missing values. This adjustment aimed to prevent these values from being treated as zero by the differentiation tools, a modification that could have further altered the overall dataset values.

By considering these complexities and implementing appropriate adjustments, the comparative analysis between the two gradient calculation methods provides insights into the potential impact of missing or erroneous data on the results.

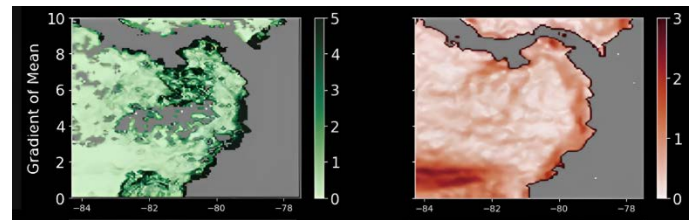


Figure 8. (a) $|\overline{\nabla chl}|$ and $|\overline{\nabla sst}|$ plotted for the subset in Figure 7

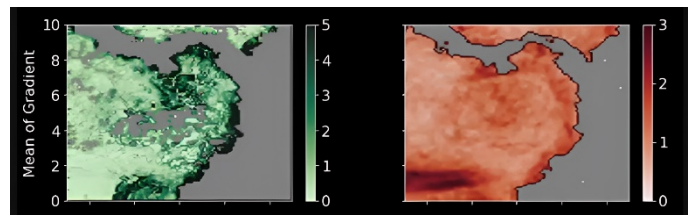


Figure 8. (b) $|\nabla \overline{chl}|$ and $|\nabla \overline{sst}|$ plotted for the subset in Figure 7

Collocating In-Situ Data with Satellite Observations

To co-locate in-situ data with satellite observations, we employed the Ocean Observatories Initiative (OOI) data, utilizing a Machine-to-Machine (M2M) approach to access data in a .json format.

The OOI THREDDS data was then transformed into a Pandas DataFrame for further analysis. Visualizations were created using Altair. The analysis centered on data retrieved from the Bulk Meteorology Instrument Package device. The utilization of Xarray facilitated the simultaneous opening of multiple files through string pattern matching.

To ensure temporal alignment, we manually provided time inputs within the designated timeframe, commencing from 12-04-2018 and ending on 10-06-2018, considering the availability of in-situ data. It is noteworthy that this timeframe was adjusted to exclude data during the periods when the Uncrewed Surface Vehicle (USV) was being hauled at the beginning and end of its cruise.

Subsequently, the cruise track of the Sairdron was plotted, encompassing measurements of chlorophyll concentration and Sea Surface Temperature (SST).

Figure 9 showcases the plotted chlorophyll data obtained from the MODIS Aqua Level 3 Standard Mapped Image Product, corresponding to the same timeframe. Similarly, Figure 10 presents the Satellite Sea Surface Temperature Data.

The initial plot utilized Multiscale Ultrahigh Resolution (MUR) SST data, which has a resolution of 0.010. However, to enhance computational efficiency, the data was updated by extracting a daily product using the NAVOCEANO repository on a 0.1° grid.

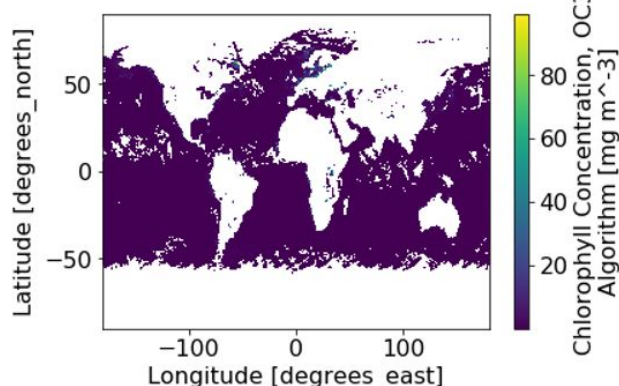


Figure 9. Chlorophyll data from MODIS Aqua Level 3 Standard Mapped Image Product.

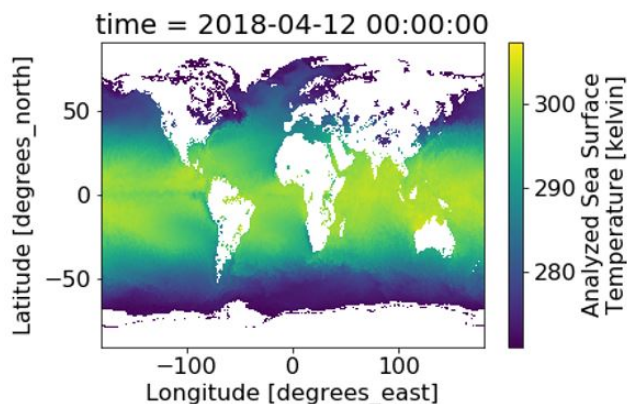


Figure 10. Sea Surface Temperature data by NAVOCEANO on a 0.1° grid

To seamlessly integrate Sairdron data with SST values, we employed Xarray interpolation techniques, ensuring accurate alignment between in-situ measurements and satellite-derived SST data. Xarray's efficient handling of multi-dimensional arrays facilitated this integration.

Figure 11 (a) and (b) vividly illustrate this integration's outcomes, showcasing chlorophyll and SST values tracked by the Sairdron's in-situ measurements. Notably, we utilized two interpolation methods³¹: (i) Linear Interpolation and (ii) Nearest Neighbor Interpolation, tailored to capture nuances in chlorophyll and Sea Surface Temperature data.

Figure 11 (a) depicts mean logarithmic chlorophyll values within a geographic scope of longitude -100 to -75 and latitude 15 to 30. Figure 11 (b) presents Sea Surface Temperature values recorded by

the Sairdron within the same region. These co-located analyses offer insights into intricate spatiotemporal chlorophyll and SST patterns, enhancing our understanding of ocean dynamics and interactions.

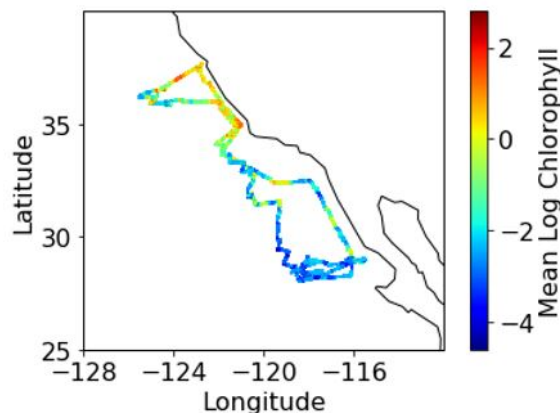


Figure 11. (a) Mean log chlorophyll value tracked by Sairdron in-situ data for lon: 75°E to 100°E , lat: 15°N to 30°N

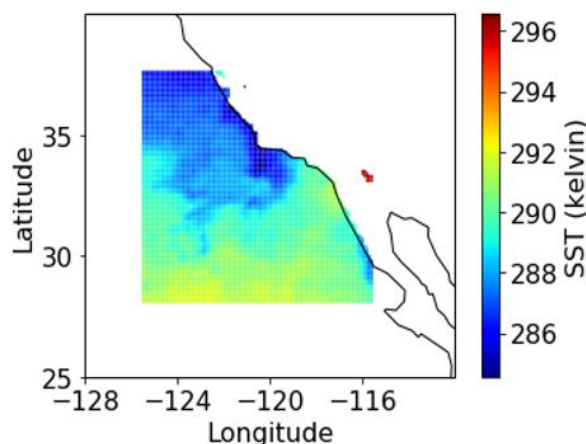


Figure 11. (b) Sea Surface Temperature values tracked by Sairdron in-situ data for lon: 75°E to 100°E , lat: 15°N to 30°N

RESULTS AND DISCUSSION

Our analysis encompasses a comprehensive exploration of water quality parameters, combining satellite observations and in-situ data to unveil intricate aquatic dynamics. In this section, we present our findings in greater detail, elucidating their significance and shedding light on their implications.

Enhancing Accuracy: Satellite Data Processing

Through a meticulous sequence of steps, we retrieved chlorophyll data from cloud storage and subjected it to a series of pre-processing stages. These stages involved sub-setting and leveraging Python tools to stack images, synchronize timeframes, and load chlorophyll data as sea surface temperature (SST) data. The resulting data were harnessed to compute spatial gradients, thereby revealing intricate spatial variations.

However, a noteworthy challenge emerged in the form of missing data points. These gaps are attributed to data points located over land or obscured by cloud cover. Presently, our analysis involves a differentiation process that "masks" these missing points

as zeros. While effective, this approach slightly impacts the reliability of gradient values, particularly near coastal regions.

Unveiling Insights: Water Surface Temperature and Algal Blooms

Water surface temperature emerges as a pivotal parameter, influencing algal blooms and climate predictions. By examining temperature patterns over time, we established a profound relationship between cyanobacterial growth and temperature fluctuations. Remarkably, our observations indicated increased algal growth during cooler periods in February and November. These blooms, while a natural phenomenon, entail consequences such as oxygen depletion, rendering the marine ecosystem unfavorable for aquatic life.

While MODIS offers reliable ocean/sea temperature data, it falls short in determining surface temperatures of inland water bodies like lakes and rivers. Multiple constraints including region restrictions, land-water boundaries, cloud cover, and rainfall contribute to data inaccuracies. Water surface temperature stands as a crucial factor in predicting algal growth trends, evident from our plots showcasing the prevalence of algal blooms during lower surface temperatures in the mentioned months.

Validation and Precision: In-Situ Data Collocation

To underscore the validity of our analysis, we aligned satellite observations with in-situ data collected by an unmanned surface vehicle (USV) Saildrone. Figures 12 (a) and (b) display the comparison results for chlorophyll concentration and sea surface temperature, respectively. To enhance the accuracy of these comparisons, we employed both linear and nearest neighbour interpolation techniques for data alignment.

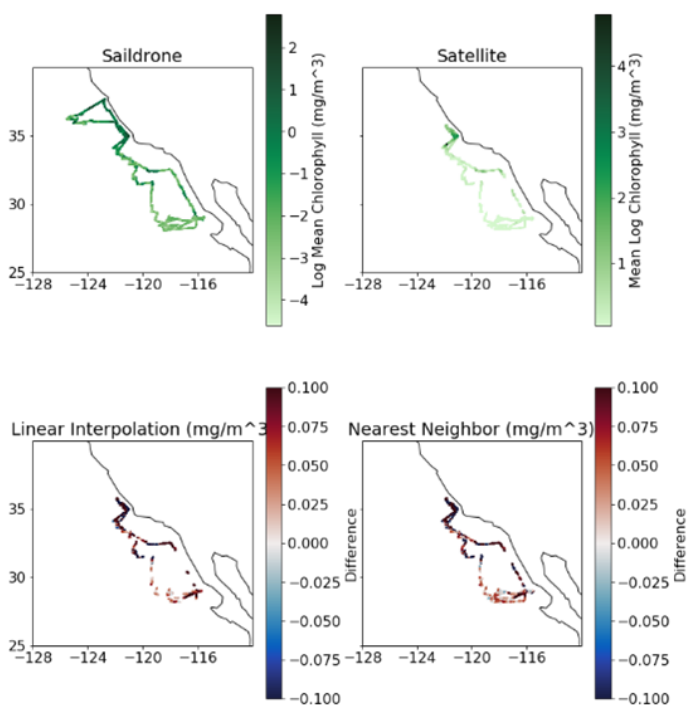


Figure 12. (a) Collocating satellite observations of chlorophyll values with in-situ data from Saildrone tracks

Moreover, we quantified the deviations between processed satellite data and in-situ measurements through mean difference

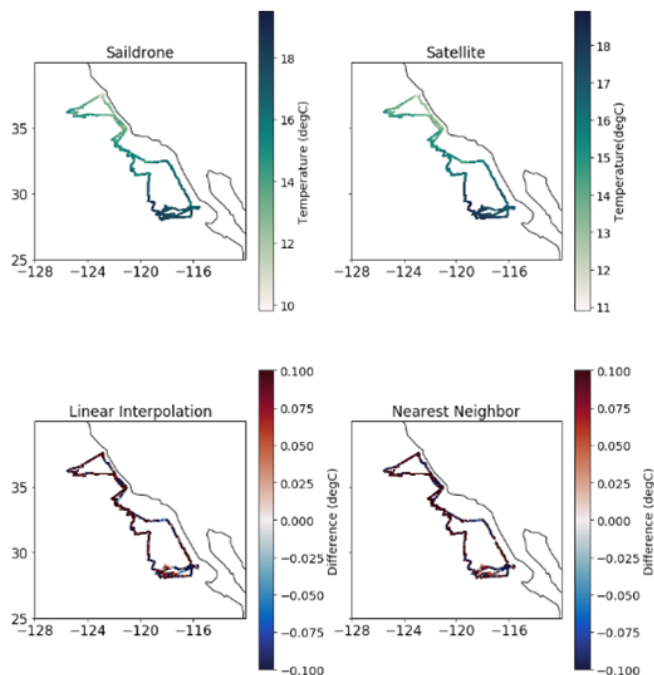


Figure 12. (b) Collocating satellite observations of SST values with in-situ data from Saildrone tracks.

and standard deviation calculations. These metrics, outlined in Table 1, provide essential insights into the agreement between the datasets. For instance, the mean difference for chlorophyll concentration was 0.0043, accompanied by a standard deviation of 0.4741. Similarly, the sea surface temperature exhibited a mean difference of 0.2054, coupled with a standard deviation of 0.4816. These discrepancies, often linked to missing values due to land or cloud cover, underscore the need for rigorous validation in satellite data analysis.

Table 1. Mean and standard deviation difference values between processed satellite data and in-situ data

Water quality parameters	Nearest neighbour interpolation		Linear interpolation	
	Mean	Standard deviation	Mean	Standard deviation
Chlorophyll Concentration	0.0043	0.4741	0.0082	0.5054
Sea Surface Temperature	0.2054	0.4816	0.2031	0.4635

CONCLUSIONS

The pursuit of remote analysis for detecting and quantifying water quality parameters through satellite data has been marked by challenges that involve intricate remote sensing techniques, diverse datasets, and complex algorithms. Historically, the field has grappled with computationally intensive and time-consuming methods, encompassing in-situ data analysis and modular client platforms for satellite image analysis. In response to this landscape, we introduced a streamlined and effective python-based framework, designed for water quality parameter analysis,

featuring key parameters like Chlorophyll concentration and Sea Surface Temperature.

Our framework leveraged open-source satellite data from a remote server, specifically the MODIS Aqua Level-3 satellite dataset. With this dataset, we orchestrated a series of data processing and analysis steps. We created time-variant maps depicting chlorophyll concentration and computed mean gradients, culminating in valuable insights into spatiotemporal trends.

Significantly, our methodology navigated challenges tied to noise inherent in satellite data, particularly land and cloud cover distortions that skewed values. To address this, we set a 90th percentile spatial gradient tolerance, a crucial decision in preserving data integrity. This approach allowed us to circumvent the loss of data points due to differentiation, especially pronounced near coastal regions. By opting to average the data rather than setting masked points as zero, we ensured a more accurate analysis.

Our study further delved into the alignment of satellite data with in-situ measurements, gauging the deviations between the two through linear and nearest neighbor interpolation techniques. This holistic approach establishes a foundation for more advanced analyses, offering both empirical and reliable insights into water quality parameters.

As our framework advances, the spectrum of analyzable parameters broadens. The future holds promise for the determination of parameters like oil spills, total dissolved matter, and dissolved organic matter with enhanced accuracy. Trends in these parameters can be probed over time to predict and anticipate changes, forging a comprehensive understanding of aquatic ecosystems. The amalgamation of various parameters, interconnected through time-corrected satellite images, stands as a potent avenue for comprehensive water quality assessment. This work thus acts as a stepping stone towards more intricate and impactful satellite-based analyses.

CONFLICT OF INTEREST STATEMENT

The authors declare that they have no conflicts of interest. No financial, professional, or personal relationships have affected the design, execution, analysis, or reporting of this study.

ACKNOWLEDGEMENT

Authors would like to thank the anonymous reviewers and the editors for their comments.

REFERENCES

1. Water Quality Monitoring: a Practical Guide to the Design and Implementation of Freshwater Quality Studies and Monitoring Programmes; Bartram, J., Ballance, R., Eds.; **1996**.
2. S.C.J. Palmer, T. Kutser, P.D. Hunter. Remote sensing of inland waters: Challenges, progress and future directions. *Rem Sens. Env.* **2015**, 157, 1–8.
3. N. Usali, M.H. Ismail. Use of Remote Sensing and GIS in Monitoring Water Quality. *J. Sustainable Develop.* **2010**, 3 (3).
4. R.P. Singh, P.K. Gupta. Developments in Remote Sensing Techniques for Hydrological Studies. *Proc. Ind. Nat. Sci. Acad.* **2016**, 82 (3).
5. J.C. Ritchie, P.V. Zimba, J.H. Everitt. Remote Sensing Techniques to Assess Water Quality. *Photogrammetric Engineering & Remote Sensing* **2003**, 69 (6), 695–704.
6. O. Dubovik, G.L. Schuster, F. Xu, Y. Hu, H. Bösch, J. Landgraf, Z. Li. Grand Challenges in Satellite Remote Sensing. *Front. Remote Sensing* **2021**, 2, 619818.
7. B. Zhang et al. Progress and Challenges in Intelligent Remote Sensing Satellite Systems. *IEEE J. Selected Topics in Applied Earth Observations and Remote Sensing* **2022**, 15, 1814–1822.
8. LAADS DAAC – NASA. Data Access Online: <https://ladsweb.modaps.eosdis.nasa.gov>. [Accessed: Dec-2019]
9. J.E. O'Reilly, P.J. Werdell. Chlorophyll algorithms for ocean color sensors – OC4, OC5 & OC6. *Remote Sensing of Environment* **2019**, 229, 32–47.
10. Ocean Data Home. NASA. Data Access Online: <https://oceandata.sci.gsfc.nasa.gov>. [Accessed: Jan-2020]
11. NetCDF: <https://doi.org/10.5065/D6H70CW6> [Accessed: June 2020]
12. S. Hoyer & J. Hamman. xarray: N-D labeled Arrays and Datasets in Python. *J. Open Research Software* **2017**, 5 (1), 10.
13. S. Hafeez, M.S. Wong, S. Abbas, et al. Detection and Monitoring of Marine Pollution Using Remote Sensing Technologies. In *Monitoring Marine Pollution*. **2018**. Intech Open.
14. Z. Chen, C. Hu, F. Muller-Karger. Monitoring turbidity in Tampa Bay using MODIS/Aqua 250-m imagery. *Remote Sens. Env.* **2007**, 109 (2), 207–220.
15. M. Gholizadeh, A. Melesse, L. Reddi. A Comprehensive Review on Water Quality Parameters Estimation Using Remote Sensing Techniques. *Sensors* **2016**, 16 (8), 1298.
16. G. Yang, X. Wang, E. Ritchie, et al. Using 250-M Surface Reflectance MODIS Aqua/Terra Product to Estimate Turbidity in a Macro-Tidal Harbour: Darwin Harbour, Australia. *Remote Sensing* **2018**, 10 (7), 997.
17. L. Shen, H. Xu, X. Guo. Satellite remote sensing of harmful algal blooms (HABs) and a potential synthesized framework. *Sensors* **2012**, 12 (6), 7778–803.
18. D. Blondeau-Patissier, J.F.R. Gower, A.G. Dekker, S.R. Phinn, V.E. Brando. A review of ocean color remote sensing methods and statistical techniques for the detection, mapping and analysis of phytoplankton blooms in coastal and open oceans. *Prog. Oceanography* **2014**, 123, 123–144.
19. P. Chauhan, M. Mohan, R.K. Sarangi, et al. Surface chlorophyll a estimation in the Arabian Sea using IRS-P4 Ocean Colour Monitor (OCM) satellite data. *Int. J. Remote Sensing* **2002**, 23 (16), 3305–3305.
20. M.A. Shareef, A. Toumi, A. Khenchaf, M. Shareef. Prediction of water quality parameters from SAR images by using multivariate and texture analysis models. **2014**. Conf. Proceed. Of SPIE.
21. S.M. Chiswell, J. Bradford-Grieve, M.G. Hadfield, S.C. Kennan. Climatology of surface chlorophyll a, autumn-winter and spring blooms in the southwest Pacific Ocean. *J. Geophysical Res.: Oceans* **2013**, 118 (2), 1003–1018.
22. O.B. Brown and P. J. Minnet. MODIS Infrared Sea Surface Temperature Algorithm Theoretical Basis Document. Version 2.0. University of Miami, Florida. **1999**.
23. A.G. O'Carroll, E.M. Armstrong, H.M. Beggs, et al. Observational Needs of Sea Surface Temperature Front. *Mar. Sci.*, **2019**, 420.
24. Q. Vanhellemont. Automated water surface temperature retrieval from Landsat 8/TIRS. *Remote Sensing of Environment* **2020**, 237, 111518.
25. Saildrone. 2018. Saildrone Baja Field Campaign Products. Ver. 1.0. PO.DAAC, CA, USA. Dataset accessed [2020-06-12] at <https://doi.org/10.5067/SDRON-SURFO>
26. J. Vazquez-Cuervo, J. Gomez-Valdes, M. Bouali. Comparison of Satellite-Derived Sea Surface Temperature and Sea Surface Salinity Gradients Using the Saildrone California/Baja and North Atlantic Gulf Stream Deployments. *Remote Sens.* **2020**, 12, 1839.
27. Q. Cao, G. Yu, Z. Qiao. Application and recent progress of inland water monitoring using remote sensing techniques. *Environmental Monitoring and Assessment* **2023**, 195, 125.
28. NASA SeaDAS Software. Online: <https://seadas.gsfc.nasa.gov/downloads/>. [Accessed: May-June-2020]
29. Google Earth Engine Team. Google Earth Engine: A cloud-based platform for planetary-scale environmental data analysis. Online: <https://earthengine.google.com/>. [Accessed: May- June 2020]
30. GDAL Development Team. GDAL: Geospatial Data Abstraction Library. Online: <https://gdal.org/> [Accessed: May-June 2020]
31. L. Beretta, A. Santaniello. Nearest neighbor imputation algorithms: a critical evaluation. *BMC Med. Informatics Decision Making* **2016**, 16 (S3).